Dynamical Solitons and Boson Fractionalization in Cold-Atom Topological Insulators

D. González-Cuadra,[1,*] A. Dauphin,[1] P. R. Grzybowski,[2] M. Lewenstein,[1,3] and A. Bermudez[4]
[1]ICFO—Institut de Ciències Fotòniques, The Barcelona Institute of Science and Technology, Avinguda Carl Friedrich Gauss 3, 08860 Castelldefels (Barcelona), Spain
[2]Faculty of Physics, Adam Mickiewicz University, Umultowska 85, 61-614 Poznań, Poland
[3]ICREA, Lluis Companys 23, 08010 Barcelona, Spain
[4]Departamento de Física Teórica, Universidad Complutense, 28040 Madrid, Spain

(Received 5 April 2020; accepted 24 November 2020; published 23 December 2020)

We study the $\mathbb{Z}_2$ Bose-Hubbard model, a chain of interacting bosons the tunneling of which is dressed by a dynamical $\mathbb{Z}_2$ field. The interplay between spontaneous symmetry breaking (SSB) and topological symmetry protection gives rise to interesting fractional topological phenomena when the system is doped to certain incommensurate fillings. In particular, we hereby show how topological defects in the $\mathbb{Z}_2$ field can appear in the ground state, connecting different SSB sectors. These defects are dynamical and can travel through the lattice carrying both a topological charge and a fractional particle number. In the hardcore limit, this phenomenon can be understood through a bulk-defect correspondence. Using a pumping argument, we show that it survives also for finite interactions, demonstrating how boson fractionalization induced by topological defects can occur in strongly correlated bosonic systems. Our results indicate the possibility of observing this phenomenon, which appears for fermionic matter in solid-state and high-energy physics, using ultracold atomic systems.

DOI: 10.1103/PhysRevLett.125.265301

Recent progress in atomic, molecular, and optical (AMO) physics has established a new paradigm for the investigation of *quantum matter*, allowing us to address well-isolated and fully controllable quantum many-body systems [1–4]. In contrast to solid-state materials, AMO matter is controlled and probed at the single-particle level, yielding a unique experimental toolbox, as exemplified by the first demonstrations of Bose-Einstein condensation with ultracold bosons [5,6]. Additionally, Feynman's idea of a quantum simulator (QS) [7], i.e., a controllable quantum device that can be used as an efficient alternative to numerical simulations of quantum many-body problems with classical computers, was also first realized with bosonic atoms [8].

A priori, the constituents of cold-atom QSs would be fermion-boson mixtures, in order to account in particular for fermionic matter in solid-state or high-energy physics models [9,10]. A broader perspective, however, is to synthesize new forms of matter which, while capturing the essence of paradigmatic models in these two disciplines, exploit other constituents to target distinct microscopic models. Experiments with bosonic atoms have played a key role in this respect, as the control and flexibility of AMO platforms [11] has allowed us to synthesize new kinds of bosonic matter, in many cases before their fermionic counterparts, and to investigate relevant many-body phenomena. For instance, ultracold bosons have been used as QSs of topological matter: from bosonic symmetry-protected topological (SPT) phases [12–14] to bosonic Hall samples [15,16] with synthetic gauge fields [17,18]. The latter is a source of fascinating physics, leading to anyons and charge fractionalization [19]. Specifically, fractionalization occurs for interacting fermions [20] or bosons [21], either in real or synthetic 2D Hall samples. However, although fractionalization has been observed directly for electrons [22–24], the bosonic counterpart is still an open problem [25].

In contrast to anyonic statistics, fractionalization can occur in one dimension. Indeed, it was discovered precisely in this context by studying relativistic quantum field theories (QFTs) of fermions and solitons [26]. The soliton, a topological excitation that appears after a SSB process and cannot be deformed into the ground state at a finite energy cost, polarizes the fermionic vacuum leading to fractionally charged quasiparticles. This also occurs in the electron-phonon Su-Schrieffer-Heeger (SSH) model of polymers [27], or for fermionic atoms coupled to optical waveguides [28]. We note that, despite past efforts with polymers, there has not been an unambiguous direct observation of soliton-induced fractionalization [19]. For SPT phases, fractional states are expected to appear in externally adjusted static solitons, which have been studied with cold atoms [29]. The full problem, however, involves dynamical solitons and the interplay between SSB and SPT. We thus consider the questions (i) is there a bosonic counterpart of fractionalization induced by dynamical solitons, and (ii) can it be accessed with cold atoms?

To address (i)–(ii), we study the $\mathbb{Z}_2$ Bose-Hubbard model (BHM) [30–32], which extends the standard BHM [33] by making the boson tunneling depend on a secondary species. This species, localized at the lattice links and described in terms of spins, can be pictured as a truncated version of the SSH phonons [27]. We show how, for incommensurate densities, the ground-state displays topological defects, as a pair of spin solitons appear for each boson doped above half-filling. We present compelling evidence that each soliton carries half a boson, thus yielding fractionalization. Using a topological invariant, we show how the solitons interpolate between regions with different bulk topology, explaining the presence of fractional particles through topological band arguments [34,35] in the hardcore limit. Finally, we generalize to softcore bosons through a pumping protocol, where quantized transport takes place between edges and solitons.

The model.—We consider bosonic fields on a chain $b_i, b_i^\dagger$, interacting locally with strength U, and coupled to $\mathbb{Z}_2$ Ising fields $\sigma^x_{i,i+1}, \sigma^z_{i,i+1}$ [Fig. 1(a)]. The link spins dress the boson tunnelling t with a strength α, and are subjected to transverse (longitudinal) fields $\beta(\Delta)$, yielding

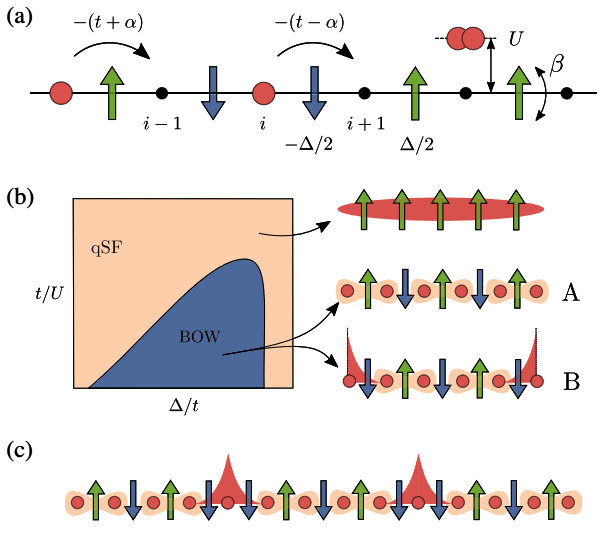

FIG. 1. *Bosonic Peierls transition and topological defects:* (a) Sketch of the $\mathbb{Z}_2$ BHM [Eq. (1)], where bosonic particles (red spheres) tunnel between different sites with a strength that depends on the $\mathbb{Z}_2$ fields (arrows) located on the bonds. (b) Qualitative phase diagram at half filling [30]. The $\mathbb{Z}_2$ fields are polarized for weak Hubbard interactions, but order antiferromagnetically if the interactions are strong enough, according to two degenerate patterns (A and B). The SSB drives the bosons from a qSF to a BOW phase, where the bosonic tunneling is dimerized (stronger tunneling in yellow). Additionally, the B SSB sector hosts a SPT phase with localized edge states (red peaks in the figure). (c) Extra bosons create pairs of topological defects in the Néel ground state, interpolating between the different SSB sectors and hosting fractionalized particles.

$$H = -\sum_{i=1}^{N} (b_i^\dagger (t + \alpha\sigma^z_{i,i+1}) b_{i+1} + \text{H.c.}) + \frac{U}{2}\sum_{i=1}^{N} b_i^\dagger b_i^\dagger b_i b_i + \frac{\Delta}{2}\sum_{i=1}^{N}\sigma^z_{i,i+1} + \beta\sum_{i=1}^{N}\sigma^x_{i,i+1}. \quad (1)$$

When considering the spin Hilbert space as a truncation of the phononic one, Eq. (1) resembles the SSH model [27] with α playing the role of the electron-phonon coupling, and Δ, β mimicking the mass and stiffness of the vibrating ions. In the SSH model, the fermionic nature of the electrons is crucial for the Peierls' instability [36], which is the precursor to solitons and fractionalization [27]. The former implies the spontaneous breaking of the system's translational invariance, giving rise to long-range order and a gap opening around the Fermi surface. Although for various fractional fillings and $U \ll t$, the $\mathbb{Z}_2$ BHM contains quasisuperfluid (qSF) phases [30–32] similar to those of the standard BHM [33], a bosonic analog of the Peierls' instability arises as the interactions are increased, despite the absence of a Fermi surface [Fig. 1(b)]. Depending on the spin fluctuations, controlled by β/Δ, ground states with coexisting magnetic long-range orders and bosonic SPT phases can be found. In this work, we explore incommensurate fillings, the existence of solitons, and the possibility of observing boson fractionalization.

This possibility is motivated by an implementation with atomic mixtures in optical lattices. The Ising spins arise from a deeply trapped atomic species with two internal states, initially prepared so as to avoid double occupancies. The bosons stem from a different atomic species, trapped by a shallower lattice, and leading to intra- and interspecies scattering described by contact density-density interactions. The spin-mediated tunneling arises as the only possible process allowed by the energetic constraints imposed by a superlattice structure. By defining the Ising spins in terms of localized atoms in nonoverlapping pairs of sites [37], and making them dynamical by means of a Floquet driving [38], one obtains a QS of the $\mathbb{Z}_2$ BHM [39].

Ground-state Ising solitons.—The above Hamiltonian has been studied at commensurate fillings [31,32], this is, at rational fractions in the thermodynamic limit. Since there are two SSB configurations for the spins, called A and B in Fig. 1(b), one envisages situations where the spins interpolate between them forming a soliton [Fig. 1(c)]. These finite-energy excitations could be created by crossing the Peierls transition dynamically [40–42]. In this work, we show that solitons also appear in the ground state for incommensurate fillings. To analyze this situation, we perform simulations based on matrix product states [43], fixing the bond dimension to $D = 100$ and the maximum boson number per site to $n_0 = 2$, which suffices for strong interactions, low densities, and $\alpha = 0.5t$.

The SSB yields Néel ordering $\langle\sigma^z_{i,i+1}\rangle = (-1)^i\varphi(i)$, where $\varphi(i)$ is a slowly varying field. The order parameter $\varphi = \sum_i \varphi(i)/N$ characterizes the two possible SSB sectors $\varphi = \pm 1$, whereas solitons correspond to a scalar field $\varphi(i)$ interpolating between them. As shown in Fig. 2, solitons present the same profile as kinks in $\lambda\varphi^4$ relativistic QFT [44], namely,

$$\varphi(i) = \tanh\left(\frac{i - i_p}{\xi}\right), \tag{2}$$

where i_P is the soliton center and ξ its width. By analogy with the scalar QFT [45], the topological charge $Q = \frac{1}{2}\int dx \partial_x \varphi(x)$ can be evaluated by a finite difference

$$Q = \frac{1}{2}[\varphi(i_p + r) - \varphi(i_p - r)], \tag{3}$$

at points well separated from the soliton center $r/\xi \sim \mathcal{O}(N)$.

Figures 2(a)–2(b) correspond to the $\beta = 0$ limit, where the spins have no quantum fluctuations, and the solitons reduce to domain walls located anywhere in the lattice. A topological charge of $Q = +1$ can be directly read from the soliton of Fig. 2(b). We remark on two differences with respect to relativistic QFT: our solitons (i) appear directly in the ground state, and (ii) are not free to move due to Peierls-Nabarro barriers, this is, to the energy difference of a soliton located at different elements of the two-site unit cell, caused by the lack of a continuous translational invariance [46,47]. In the following, we use the term *antisoliton* to denote defects with $Q = -1$, as these can annihilate

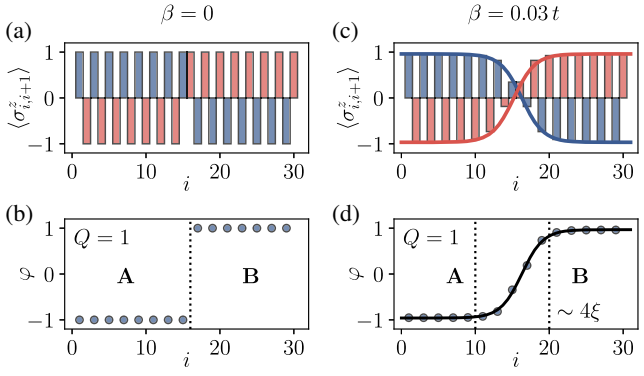

FIG. 2. *Ising topological defects:* We show the ground state configuration for a chain of $N = 31$ sites and $N_b = 16$ bosons, with $U = 10t$ and $\Delta = 0.80t$, where a topological defect appears in the dimerized pattern of the $\mathbb{Z}_2$ fields. (a) and (b) show the magnetization $\langle\sigma^z_{i,i+1}\rangle$ and the order parameter φ_j for $\beta = 0$, respectively, where the defect is a domain wall with topological charge $Q = 1$ (3). (c)–(d) Analogous topological defect for $\beta = 0.03t$, where quantum fluctuations broaden the defect, leading to a soliton of finite width ξ, that can be accurately fitted to Eq. (2).

together with $Q = 1$ solitons forming configurations with zero topological charge.

As $\beta > 0$ is switched on, the Ising spins are no longer classical discrete variables, but become dynamical fluctuating fields. A direct consequence is that they can tunnel through the barriers and delocalize. To benchmark the prediction (2), we introduce a pinning mechanism by raising $\beta \to \beta_0 = \beta(1 + \epsilon)$ at two consecutive bonds surrounding the pinning center i_p. The soliton can be pinned anywhere in the chain to study its intrinsic properties. In Figs. 2(c)–2(d), we show that quantum fluctuations widen the extent of the soliton, where the nonzero width $\xi > 0$ is extracted by fitting the corresponding slowly varying field $\varphi(i)$ to Eq. (2). In Ref. [39], we discuss in more detail the aforementioned Peierls-Nabarro barriers, and the widening of the soliton, paying special attention to the role of the Hubbard interactions which control the backaction of the bosonic matter on the solitons. Moreover, we also explore incommensurate fillings around densities $1/3$ and $2/3$, which lead to solitons with higher topological charges. We expect similar phenomena around other rational densities with more complicated long-range orders.

Fractionalization of bosons.—The fact that solitons are not restricted to finite-energy excitations but appear in the ground state is crucial to find a bosonic version of charge fractionalization. We find an unambiguous manifestation of this effect by doping the half-filled system with a single particle. To accommodate for this particle, an Ising soliton or antisoliton pair is created, each hosting a bound quasiparticle with a fractionalized number of bosons, i.e., the boson splits into two halves. The same pair will be created also if one boson is subtracted from half filling, where now each defect hosts half a bosonic hole with negative particle number. This mechanism is confirmed by Fig. 3. The order-parameter field displays the aforementioned soliton-antisoliton pair for a chain of $N = 90$ sites and filled with $N_b = 46$ bosons [Figs. 3(a) and 3(d)]. One clearly sees that there is a density build-up around the topological defects that follows the superposition of two profiles

$$\langle{:}n_j{:}\rangle = \langle n_j\rangle - \frac{1}{2} = \frac{1}{4\xi}\mathrm{sech}^2\left(\frac{j - j_p}{\xi}\right), \tag{4}$$

for the even $j = 2i$ or odd $j = 2i + 1$ sublattices, with their corresponding centers j_p being fixed by the soliton-antisoliton positions. We note that this expression coincides with the profile of fermionic zero modes for the relativistic Jackiw-Rebbi model [48,49], where fractionalization was first predicted [26].

To test if bosons fractionalize, Figs. 3(b) and 3(e) present the integrated density $N_i = \sum_{j\le i}\langle{:}n_j{:}\rangle$, which shows two plateaus where the boson charge jumps by steps of $1/2$. Accordingly, the soliton and antisoliton bind half a boson each, forming two fractionalized quasiparticles. Both the

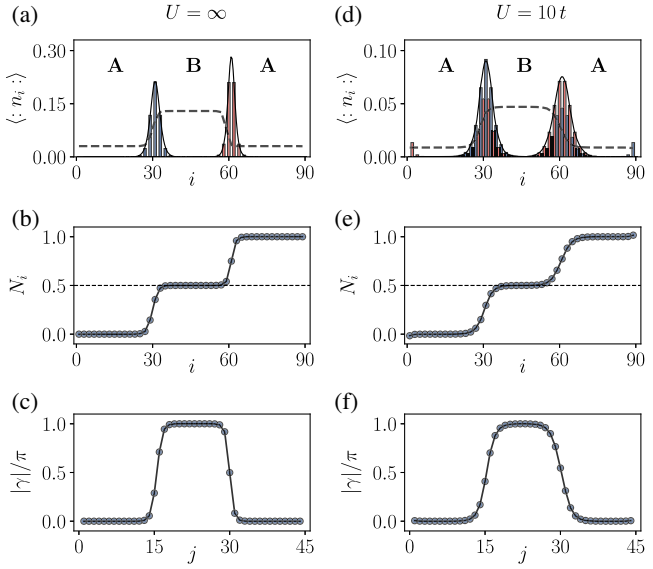

FIG. 3. *Boson fractionalization and local Berry phase:* (a) Occupation number $\langle : n_i : \rangle$ for a chain with $N = 90$ sites and $N_b = 46$ hardcore bosons, for $\Delta = 0.70t$ and $\beta = 0.03t$. We superimpose φ using dashed lines. We observe peaks in the occupation at the defects, localized on different sub-lattices (blue and red). The solid lines correspond to a fit to Eq. (4). (b) The integrated particle number N_i shows how each peak contains half a particle. (c) The local Berry phase γ is quantized to 0 or π in the different SSB sectors, and interpolates between the two around the defects. (d) Softcore bosons with $U = 10t$, $\Delta = 0.80t$ and $\beta = 0.02t$, where we still observe peaks in the occupation. These have now support on both sublattices, since chiral symmetry is broken, but are still associated with fractionalized bosons (e).(f) The topological Berry phase is also quantized since inversion symmetry is preserved.

soliton profiles and fractionalization could be detected experimentally by measuring the local atomic occupation with a quantum gas microscope [50,51]. This contrasts with the complications for site-resolved measurements in the solid state, which have hindered the direct observation of soliton-induced fractionalization.

In the companion article [39], we present an in-depth analysis of this fractionalization phenomenon, ruling out the existence of polaron quasiparticles, and showing that the soliton dynamics is crucial to understand the appearance of self-assembled soliton lattices with a periodic arrangement of the fractional charges. Moreover, we extend the analysis to doping above other commensurate fillings, where the larger topological charges allow for other fractionalization patterns.

Many-body topological invariants.—The topological characterization is not fully captured by the topological charge of the order-parameter field (3). In particular, the bosonic sector may also display a topological Berry phase, the calculation of which requires a full quantum-mechanical treatment,

$$\gamma_i = \int_0^{2\pi} d\theta_i \langle \epsilon_{\rm gs}(\theta_i) | \mathrm{i}\partial_{\theta_i} | \epsilon_{\rm gs}(\theta_i) \rangle, \tag{5}$$

where θ_i is the angle that twists the bosonic tunneling $t \to te^{\mathrm{i}\theta_i}$ between i and $i+1$, and $|\epsilon_{\rm gs}(\theta_i)\rangle$ is the corresponding ground state. This local Berry phase generalizes the notion of a many-body Berry phase with twisted boundary conditions [52], and can be applied to non-translationally invariant situations [53].

In Figs. 3(c) and 3(f), one can see how the intercell local Berry phase changes by $\Delta\gamma = \pm\pi$ as one traverses the soliton or antisoliton. Therefore, the topological defects not only carry a topological charge $Q = \pm 1$, but they separate topologically trivial regions $\gamma_A = 0$ from nontrivial ones $\gamma_B = \pi$. We note that the theory of defects in SPT phases [34,35] relates such inhomogeneous layouts of topological invariants with the existence of protected quasiparticles localized at the defects, a relation known as the bulk-defect correspondence.

We emphasize, however, that this theory deals with fermions and assumes an externally adjusted defect, which only serves to provide a background for the fermions. To our knowledge, our results show for the first time that analogous effects occur for bosons in a fully fledged quantum many-body problem where the defects are dynamically fluctuating solitons. Following this connection, we note that in the $U/t \to \infty$ limit, the $\mathbb{Z}_2$ BHM has an additional chiral symmetry, and the corresponding localized quasiparticles have support in just one of the two sublattices [Fig. 3(c)]. Therefore, apart from the inherent robustness of the classical solitons, the total defects formed by a soliton and a fractionalized boson are also protected against chiral-preserving perturbations.

Quantized boson transport between edges and defects.—For a finite value of U/t, this chiral symmetry is broken and, although the phase remains topological—protected now by inversion symmetry [31]—the quantized value of the Berry phase shown in Fig. 3(f) does not imply a topological protection of the localized states. However, here we show how the quantized intersoliton and edge-soliton transport of bosons is topologically protected, and that the localized quasiparticles can be understood as the remnants of higher-dimensional states that do have this additional robustness. To see this, we induce a Thouless pumping by driving the Ising fields along a periodic cycle $\Delta \to \Delta_i(\phi) = 2(-1)^i t\cos\phi, \quad \beta \to \beta_i(\phi) = (-1)^i t\sin\phi$, where ϕ: $0 \to 2\pi$.

In fermionic SPT phases, such adiabatic cycles lead to the transport of an integer number of fermions Δn across the system, which coincides with the Chern number $\Delta n = \nu$ of an effective 2D system [54]. Alternatively [55,56], this invariant can be obtained from the change of the Berry phase,

$$\nu = \frac{1}{2\pi}\int_0^{2\pi} d\phi \partial_\phi \gamma(\phi). \tag{6}$$

As shown in Figs. 4(a)–4(b), the change of the local Berry phase at the middle of the chain yields the Chern numbers

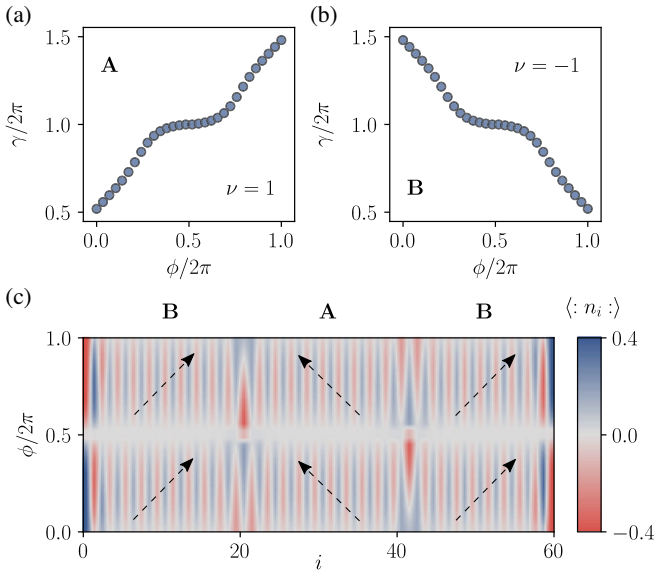

FIG. 4. *Bosonic pumping between edges and defects:* We show how the Berry phase γ changes with the pumping parameter ϕ, calculated at the middle of a chain with $N = 42$ and $N_b = 21$. The change in this quantity (6) is associated to the Chern number of an extended 2D system, where (a) and (b) correspond to the 1D configurations A and B, respectively, at $\phi = 0$. (c) Bosonic occupation $\langle : n_i : \rangle$ through the pumping cycle of a system with two domain walls, starting from a BAB configuration at $\phi = 0$. Each region transports a quantized charge in the bulk given by $\Delta n = -\nu$. The arrows denote the direction of the pumped charge, flowing between edges and defects.

$\nu = \pm 1$ depending on the SSB sector A/B of the initial state. By calculating the evolution of the boson density [Fig. 4(c)], one clearly observes that a single bosonic charge is transferred between the soliton and antisoliton, and between each of them and the closest edge. Comparing with Figs. 4(a)–4(b), it becomes clear that this pumping is directly associated with the different Chern numbers. As announced above, the fractional bosons bound to the defects can be understood as remnants of the higher-dimensional conducting states that are localized at the interfaces separating the 2D regions of different Chern number. This establishes a generalized bulk-boundary correspondence in the absence of chiral symmetry where, even if the observed fractional states at the defects are not protected, they contribute to topologically protected transport properties, and these can be inferred from the topological properties of the bulk. In the companion paper [39], we give more details of this pumping, showing that it is crucial to understand the topological properties of the soliton quasiparticles that appear at other fractional fillings even in the hardcore limit.

Conclusions and outlook.—We showed how boson fractionalization induced by dynamical solitons can take place in cold-atomic systems. In particular, we study the ground state of the $\mathbb{Z}_2$ BHM for incommensurate densities around half filling. We found composite quasiparticles consisting on dynamical solitons bound to fractional bosons, and characterized their topological properties and fractional charges. Finally, we connected these properties to the topological character of the underlying bulk through a generalized bulk-defect correspondence and the quantization of intersoliton transport.

This project has received funding from the European Union Horizon 2020 research and innovation programme under the Marie Skłodowska-Curie Grant Agreement No. 665884, the Spanish Ministry MINECO and State Research Agency AEI (FIDEUA PID2019-106901GB-I00/10.13039/501100011033, SEVERO OCHOA No. SEV-2015-0522 and CEX2019-000910-S, FPI), ERC AdG NOQIA, European Social Fund, Fundació Cellex, Fundació Mir-Puig, Generalitat de Catalunya (AGAUR Grant No. 2017 SGR 1341, CERCA program, QuantumCAT_U16-011424, co-funded by ERDF Operational Program of Catalonia 2014–2020), MINECO-EU QUAN-TERA MAQS (funded by The State Research Agency (AEI) PCI2019-111828-2/10.13039/501100011033), and the National Science Centre, Poland-Symfonia Grant No. 2016/20/W/ST4/00314. A. D. acknowledges the financial support from a fellowship granted by la Caixa Foundation (ID 100010434, fellowship code LCF/BQ/PR20/11770012). A. B. acknowledges support from the Ramón y Cajal program RYC-2016-20066, and CAM/FEDER Project No. S2018/TCS-4342 (QUITEMAD-CM) and the Plan Nacional Generación de Conocimiento PGC2018-095862-B-C22.

*daniel.gonzalez@icfo.eu

[1] M. Lewenstein, A. Sanpera, and V. Ahufinger, *Ultracold Atoms in Optical Lattices: Simulating Quantum Many-body Systems* (Oxford University Press, Oxford, 2017).
[2] C. Gross and I. Bloch, Science **357**, 995 (2017).
[3] N. Goldman, J. C. Budich, and P. Zoller, Nat. Phys. **12**, 639 (2016).
[4] F. Schäfer, T. Fukuhara, S. Sugawa, Y. Takasu, and Y. Takahashi, Nat. Rev. Phys. **2**, 411 (2020).
[5] E. A. Cornell and C. E. Wieman, Rev. Mod. Phys. **74**, 875 (2002).
[6] W. Ketterle, Rev. Mod. Phys. **74**, 1131 (2002).
[7] R. P. Feynman, Int. J. Theor. Phys. **21**, 467 (1982).
[8] M. Greiner, O. Mandel, T. Esslinger, T. W. Hänsch, and I. Bloch, Nature (London) **415**, 39 (2002).
[9] M. Lewenstein, A. Sanpera, V. Ahufinger, B. Damski, A. Sen(De), and U. Sen, Adv. Phys. **56**, 243 (2007).
[10] M. C. Bauls, R. Blatt, J. Catani, A. Celi, J. I. Cirac, M. Dalmonte, L. Fallani, K. Jansen, M. Lewenstein, S. Montangero, C. A. Muschik, B. Reznik, E. Rico, L. Tagliacozzo, K. V. Acoleyen, F. Verstraete, U. J. Wiese, M. Wingate, J. Zakrzewski, and P. Zoller, arXiv:1911.00003.
[11] I. Bloch, J. Dalibard, and W. Zwerger, Rev. Mod. Phys. **80**, 885 (2008).

[12] M. Atala, M. Aidelsburger, J. T. Barreiro, D. Abanin, T. Kitagawa, E. Demler, and I. Bloch, Nat. Phys. **9**, 795 (2013).

[13] E. J. Meier, F. A. An, A. Dauphin, M. Maffei, P. Massignan, T. L. Hughes, and B. Gadway, Science **362**, 929 (2018).

[14] S. de Léséleuc, V. Lienhard, P. Scholl, D. Barredo, S. Weber, N. Lang, H. P. Büchler, T. Lahaye, and A. Browaeys, Science **365**, 775 (2019).

[15] M. Aidelsburger, M. Atala, M. Lohse, J. T. Barreiro, B. Paredes, and I. Bloch, Phys. Rev. Lett. **111**, 185301 (2013).

[16] H. Miyake, G. A. Siviloglou, C. J. Kennedy, W. C. Burton, and W. Ketterle, Phys. Rev. Lett. **111**, 185302 (2013).

[17] Y. J. Lin, R. L. Compton, K. Jiménez-García, J. V. Porto, and I. B. Spielman, Nature (London) **462**, 628 (2009).

[18] M. Aidelsburger, M. Atala, S. Nascimbène, S. Trotzky, Y.-A. Chen, and I. Bloch, Phys. Rev. Lett. **107**, 255301 (2011).

[19] R. B. Laughlin, Rev. Mod. Phys. **71**, 863 (1999).

[20] R. B. Laughlin, Phys. Rev. Lett. **50**, 1395 (1983).

[21] N. R. Cooper, N. K. Wilkin, and J. M. F. Gunn, Phys. Rev. Lett. **87**, 120405 (2001).

[22] V. J. Goldman and B. Su, Science **267**, 1010 (1995).

[23] L. Saminadayar, D. C. Glattli, Y. Jin, and B. Etienne, Phys. Rev. Lett. **79**, 2526 (1997).

[24] R. de Picciotto, M. Reznikov, M. Heiblum, V. Umansky, G. Bunin, and D. Mahalu, Nature (London) **389**, 162 (1997).

[25] N. R. Cooper, in *Fractional Quantum Hall Effects*, edited by B. I. Halperin and J. K. Jain (World Scientific, Singapore, 2020).

[26] R. Jackiw and C. Rebbi, Phys. Rev. D **13**, 3398 (1976).

[27] W. P. Su, J. R. Schrieffer, and A. J. Heeger, Phys. Rev. Lett. **42**, 1698 (1979).

[28] K. A. Fraser and F. Piazza, Commun. Phys. **2**, 48 (2019).

[29] E. J. Meier, F. A. An, and B. Gadway, Nat. Commun. **7**, 13986 (2016).

[30] D. González-Cuadra, P. R. Grzybowski, A. Dauphin, and M. Lewenstein, Phys. Rev. Lett. **121**, 090402 (2018).

[31] D. González-Cuadra, A. Dauphin, P. R. Grzybowski, P. Wójcik, M. Lewenstein, and A. Bermudez, Phys. Rev. B **99**, 045139 (2019).

[32] D. González-Cuadra, A. Bermudez, P. R. Grzybowski, M. Lewenstein, and A. Dauphin, Nat. Commun. **10**, 2694 (2019).

[33] M. P. A. Fisher, P. B. Weichman, G. Grinstein, and D. S. Fisher, Phys. Rev. B **40**, 546 (1989).

[34] J. C. Y. Teo and C. L. Kane, Phys. Rev. B **82**, 115120 (2010).

[35] J. C. Teo and T. L. Hughes, Annu. Rev. Condens. Matter Phys. **8**, 211 (2017).

[36] R. Peierls, *Quantum Theory of Solids*, International Series of Monographs on Physics (Clarendon Press, Oxford, 1955).

[37] L. Barbiero, C. Schweizer, M. Aidelsburger, E. Demler, N. Goldman, and F. Grusdt, Sci. Adv. **5**, eaav7444 (2019).

[38] A. Eckardt, Rev. Mod. Phys. **89**, 011004 (2017).

[39] D. González-Cuadra, A. Dauphin, P. R. Grzybowski, M. Lewenstein, and A. Bermudez, companion paper, Phys. Rev. B **102**, 245137 (2020).

[40] T. W. B. Kibble, J. Phys. A **9**, 1387 (1976).

[41] W. H. Zurek, Nature (London) **317**, 505 (1985).

[42] W. H. Zurek, U. Dorner, and P. Zoller, Phys. Rev. Lett. **95**, 105701 (2005).

[43] J. Hauschild and F. Pollmann, SciPost Phys. Lect. Notes 5 (2018).

[44] R. F. Dashen, B. Hasslacher, and A. Neveu, Phys. Rev. D **10**, 4130 (1974).

[45] R. Rajaraman, *Solitons and Instantons. An Introduction to Solitons and Instants in Quantum Field Theory* (North-Holland, Amsterdam, 1982), p. 409.

[46] R. Peierls, Proc. Phys. Soc. London **52**, 34 (1940).

[47] F. R. N. Nabarro, Proc. Phys. Soc. London **59**, 256 (1947).

[48] D. K. Campbell and A. R. Bishop, Phys. Rev. B **24**, 4859 (1981).

[49] D. González-Cuadra, A. Dauphin, M. Aidelsburger, M. Lewenstein, and A. R. Bermudez, arXiv:2008.02045.

[50] W. S. Bakr, J. I. Gillen, A. Peng, S. Fölling, and M. Greiner, Nature (London) **462**, 74 (2009).

[51] J. F. Sherson, C. Weitenberg, M. Endres, M. Cheneau, I. Bloch, and S. Kuhr, Nature (London) **467**, 68 (2010).

[52] Q. Niu and D. J. Thouless, J. Phys. A **17**, 2453 (1984).

[53] Y. Hatsugai, J. Phys. Soc. Jpn. **75**, 123601 (2006).

[54] Q. Niu, D. J. Thouless, and Y.-S. Wu, Phys. Rev. B **31**, 3372 (1985).

[55] M. P. Zaletel, R. S. K. Mong, and F. Pollmann, J. Stat. Mech. (2014) P10007.

[56] A. Alexandradinata, T. L. Hughes, and B. A. Bernevig, Phys. Rev. B **84**, 195103 (2011).